Supplemental Material

S1 – Control of latency results for effect size

Inhomogeneity of average spike rate or effect size, e.g. differences in the neural response selectivity, could bias latency measures between different cortical areas. First, since our recruitment curves focused on only the significant neurons, different firing rates in both area could lead to a higher number of significantly tuned neurons in the area with higher firing rates due to statistical power. We analyzed firing rates in PMd and PRR on average across those neurons, which contributed to the analyses in the main text, i.e. neurons with motor-related tuning and no cue-response. For each neuron the average firing rate was determined in the same time window as was used for computing the maximum direction (MD), which was 200 to 350 ms after onset of the cue (precue in RS, go-cue in N, R, S). Firing rates in PMd during anti-trials were not significantly different from those in PRR in either cueing condition. Second, the effect size in each area was quantified with the maximum p-value for directional selectivity within the analysis time window averaged across all neurons (The negative logarithm of the p value to the basis of ten was used for statistical comparisons; p values smaller than 10^{-6} were set to 10^{-6}). There was either no significant difference in effect size between PMd and PRR (RS-pro, R-anti, S-pro) or the effect size was significantly higher ($p<0.05$, t-test) in PRR compared to PMd (RS-anti, N-pro, N-anti, R-pro and S-anti). Only in RS-anti the effect size in PMd was higher than in PRR. If at all, higher effect size in PRR should lead to opposite latency differences between both areas in most cueing conditions than the ones we found. Taken together, neither differences in average firing rate nor in average tuning strength could explain the observed LDs between PMd and PRR.

In the standard analysis neurons were included if they showed motor-related tuning at some point in time during the analysis time window. The significance criterion of being tuned ($p<0.05$ in Kruskal-Wallis test) implies an artificial threshold. As additional control we ran our analysis with different thresholds for the significance of an individual neuron's tuning ($\alpha = 0.01$, 0.1, or 0.2). In the S-pro condition the effect of LD(PRR-PMd), which only showed a non-significant trend ($p = 0.057$) in the standard analysis with tuning threshold $\alpha = 0.05$ (Fig. 3B and 6A), was significant ($p = 0.026$) when neurons were selected with a stricter significance criterion for tuning ($\alpha = 0.01$). In all other conditions the significances did not change (Fig. S-1). These findings corroborate our conclusions of the main manuscript, especially they provide evidence for earlier motor-goal representations in PMd than PRR in the S-pro condition.

S 2 – Control of latency results for sampling bias

Similar to effect size (Supplemental Material 1) differences in the size of the neuron sample between the two areas could affect latency measures based on recruitment curves. We randomly subsampled the same number of neurons in PMd and PRR (Pesaran et al. 2008), to balance the number of neurons analyzed in each area (Fig. S-2). The distributions of LDs in the different task conditions obtained from repeated random sampling of neurons were not different from the original values ($p>0.4$, confidence interval), which means the results were independent of the specific neuron samples. In summary, section 1 and 2 of Supplementary Material suggest that population size, effect size, or average spike rate differences did not confound our latency measures.

S 3 – Alternative latency measures

As an alternative latency measurement we compared the cumulative sums over all single-unit motor-related tuning onset latencies (Fig. S-3). Within each cueing condition and for each neuron the onset latency was defined as the first time point at which the tuning became motor-related and continued to do so for at least 90% of 50 consecutive time bins (equivalent to the definition of motor planning activity in the memory period of the RS condition; see Material and Methods). The time window of analysis for each cueing condition was identical to the standard analysis in the main manuscript, which was -200 ms to + 450 ms relative to the onset of the pre-cue (RS) or go-cue (N, R, S). The number of neurons which fulfilled the criterion for motor-tuning is provided in the legend of Fig. S-3. Median onset latencies for motor-tuning were lower in PMd than PRR ($p<0.01$, Wilcoxon signed rank test) in all four cueing conditions which required spatial remapping (RS-anti, N-anti, R-anti, S-pro) These results confirm the results in the main text.

S 4 – Temporary bimodal tuning properties

Population PSTHs around the time of the go-cue in the N condition (Fig. 2C) suggest that for a brief period of time, between approx. 100-250 ms after cue onset, neural activity in PMd did not only increase for reaches to the maximum direction (MD), but also for reaches to the non-preferred direction (NP). As a consequence, the separation between MD and NP PSTH curves occurred later in PMd than PRR during pro-

reaches, while the recruitment curves and statistical tests indicated synchronous onset of motor-goal tuning in PMd and PRR. Here we explain this seeming contradiction by showing that in PMd in response to the go-cue in the N condition a small fraction of neurons temporarily showed bimodal tuning, i.e. they briefly reflect both potential motor goals, the pro- and the anti-goal.

To test the significance of directional tuning in our standard analysis in the main text we used a non-parametric 1-way ANOVA with the additional criterion that the length of the normalized DTV had to be larger than 0.2. With this criterion we excluded neurons with a bipolar tuning close to symmetric (ANOVA significant, $|DTV| < 0.2$) from the recruitment curves and statistical analysis, but not from the population PSTHs. Such symmetric bipolar tuning could represent two potential motor goals instead of one selected motor goal and would be characterized by a significant ANOVA while the DTV has a length close to zero (see Material and Methods). The test for bimodality was conducted separately in pro- and anti-trials for all neurons which did not have a cue-related response. Figures S-4 A and B show the time-resolved number of bimodal neurons in PMd and PRR for the RS and N conditions. Especially in the N condition in PMd there was a clear increase in the number of bimodal neurons between 100-250 ms after cue onset, most pronounced for pro-reaches. Figure S4 C shows the tuning between 100-250 ms for PMd neurons in the N-pro condition (normalized within each neuron and averaged across neurons), which showed bimodal tuning for at least 10 time bins in this time window. The fact, that the average tuning shows opposing local maxima at 0 and 180 deg is consistent with the interpretation that the tuning reflects the encoding of two potential motor goals.

We speculate that bimodal tuning was stronger in the N condition than in the RS condition because of the time pressure for the monkey in the N condition. It takes longer to process the rule information than the spatial information (compare RTs for R and S conditions in pro-reaches, Fig. 6A). Evaluation of the spatial cue before the rule is known narrows down the choices to two out of four remaining spatial targets, the pro- and the anti-goal. Once the rule information was processed, one of the two putative activity peaks had to be suppressed (resulting in the motor-goal tuning of which we analyzed the latencies with our recruitment curves). This strategy might have been faster for the monkey than building up a new activity peak after the delayed evaluation of the transformation rule. In the RS condition after the pre-cue, there was no time pressure for the monkey and therefore no need to build up potential motor-goal tuning.

Supplemental Figures

Figure S-1: Control for the effect of tuning significance thresholds on LD measures. Frontoparietal LDs are shown for pro- (top row) and anti-trials (bottom row) in the different cueing conditions. A-C: LD results when different significance thresholds were applied to the spatial tuning of each neuron in pro- and anti-reaches. A: LDs if significance of spatial tuning in single neurons and time windows was defined by $p<0.2$ (Kruskal-Wallis). B and C: Same as A but significance defined with $p < 0.1$ and 0.01, respectively.

Figure S-2: Control for the effect of sample sizes in PMd and PRR on LD measures. Mean and standard deviation (1000 randomizations) of frontoparietal LDs for pro- (left panel) and anti-trials (right panel) in the different cueing conditions. In each randomization run a random sub-sample of the same number of neurons in PRR and PMd were taken. Asterisks indicate the level of significance (*: $p<0.05$, **: $p<0.01$). The dots indicate the original value with unequal number of neurons in PMd and PRR. The original LDs were not different from the LDs derived from balanced sample sizes ($p >0.4$).

Figure S-3: Alternative neural latency measure. The curves show cumulative sums over the onset latencies of motor-related tuning. PMd (red) and PRR (yellow) data are shown separately for pro- (left) and anti-trials (right) in the different cueing conditions (A-D). The motor-tuning onset latencies are derived for each single neuron within each condition. Additional to the cumulative sums the median onset latency and the p-value (ranksum-test) for the comparison between PMd and PRR onset latency

distribution are provided. Also, the numbers of neurons in each area are provided, for which an onset latency could be computed.

Figure S-4: Analysis of temporary bimodal tuning after cue presentation. A: Number of putatively bimodal neurons in PMd (red) and PRR (yellow) and separate for pro- (left) and anti-trials (right) in the RS-condition after onset of the precue. B: Same as in A, but in the N condition after onset of the go-cue. C: Average normalized tuning of putatively bimodal PMd neurons in pro-trials in the N condition (the condition with the strongest indication for bimodal tuning). The tuning curve is bi-lobed, indicating bimodal tuning, even though not fully symmetrically. The time window, which was used for computing the directional tuning, is indicated by the black bar in B. Data are aligned and normalized to the average maximal response in pro-trials in the time window of analysis.

Figure S-1

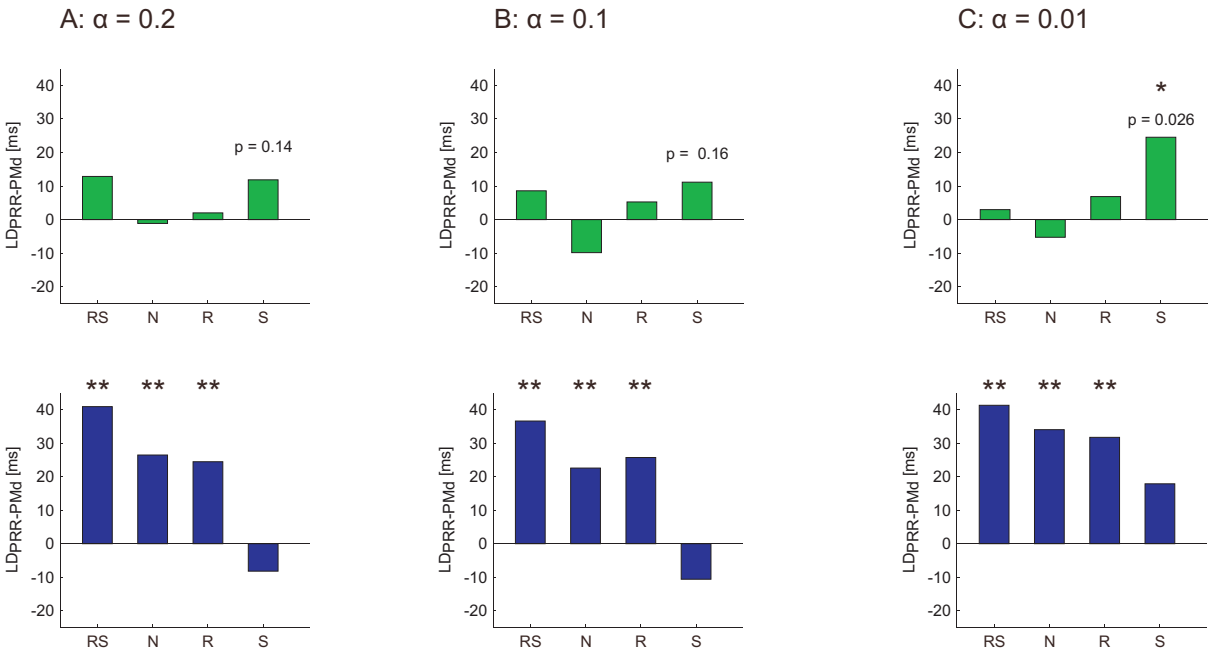

Figure S-1: Control for the effect of tuning significance thresholds on LD measures. Frontoparietal LDs are shown for pro- (top row) and anti-trials (bottom row) in the different cueing conditions. A-C: LD results when different significance thresholds were applied to the spatial tuning of each neuron in pro- and anti-reaches. A: LDs if significance of spatial tuning in single neurons and time windows was defined by $p<0.2$ (Kruskal-Wallis). B and C: Same as A but significance defined with $p < 0.1$ and 0.01, respectively.

Figure S-2

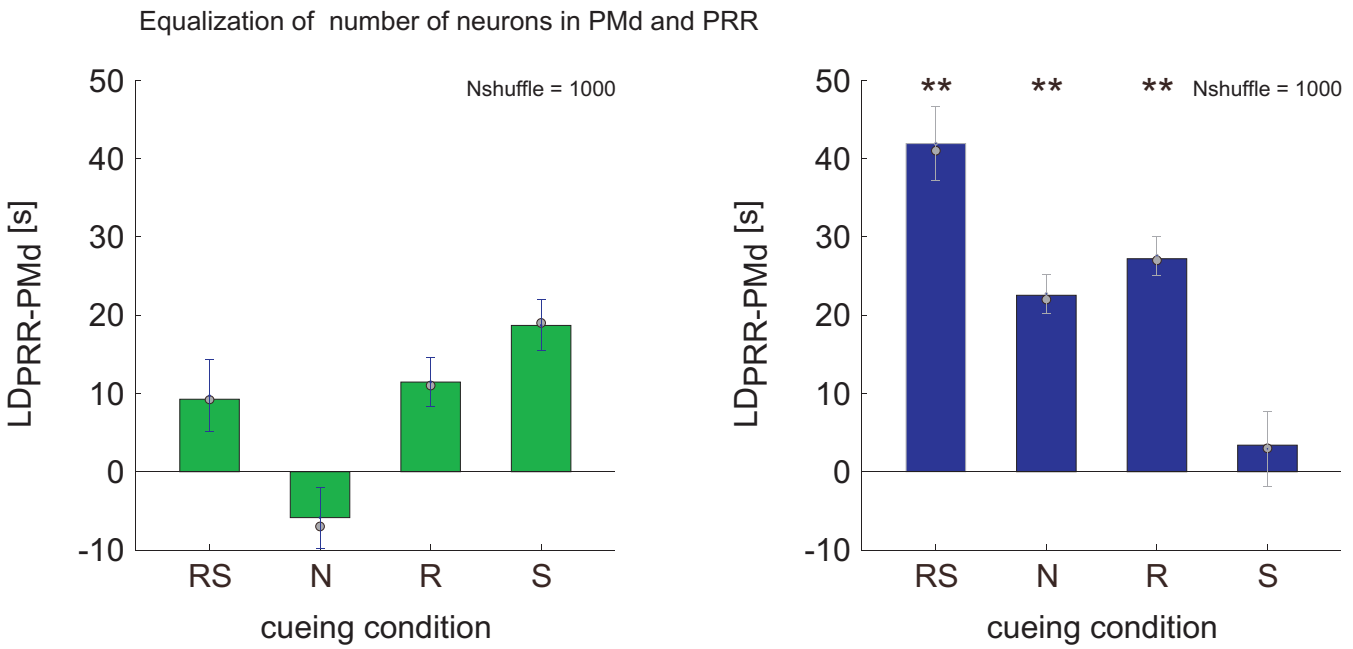

Figure S-2: Control for the effect of sample sizes in PMd and PRR on LD measures. Mean and standard deviation (1000 randomizations) of frontoparietal LDs for pro- (left panel) and anti-trials (right panel) in the different cueing conditions. In each randomization run a random sub-sample of the same number of neurons in PRR and PMd were taken. Asterisks indicate the level of significance (*: $p<0.05$, **: $p<0.01$). The dots indicate the original value with unequal number of neurons in PMd and PRR. The original LDs were not different from the LDs derived from balanced sample sizes ($p>0.4$).

Figure S-3

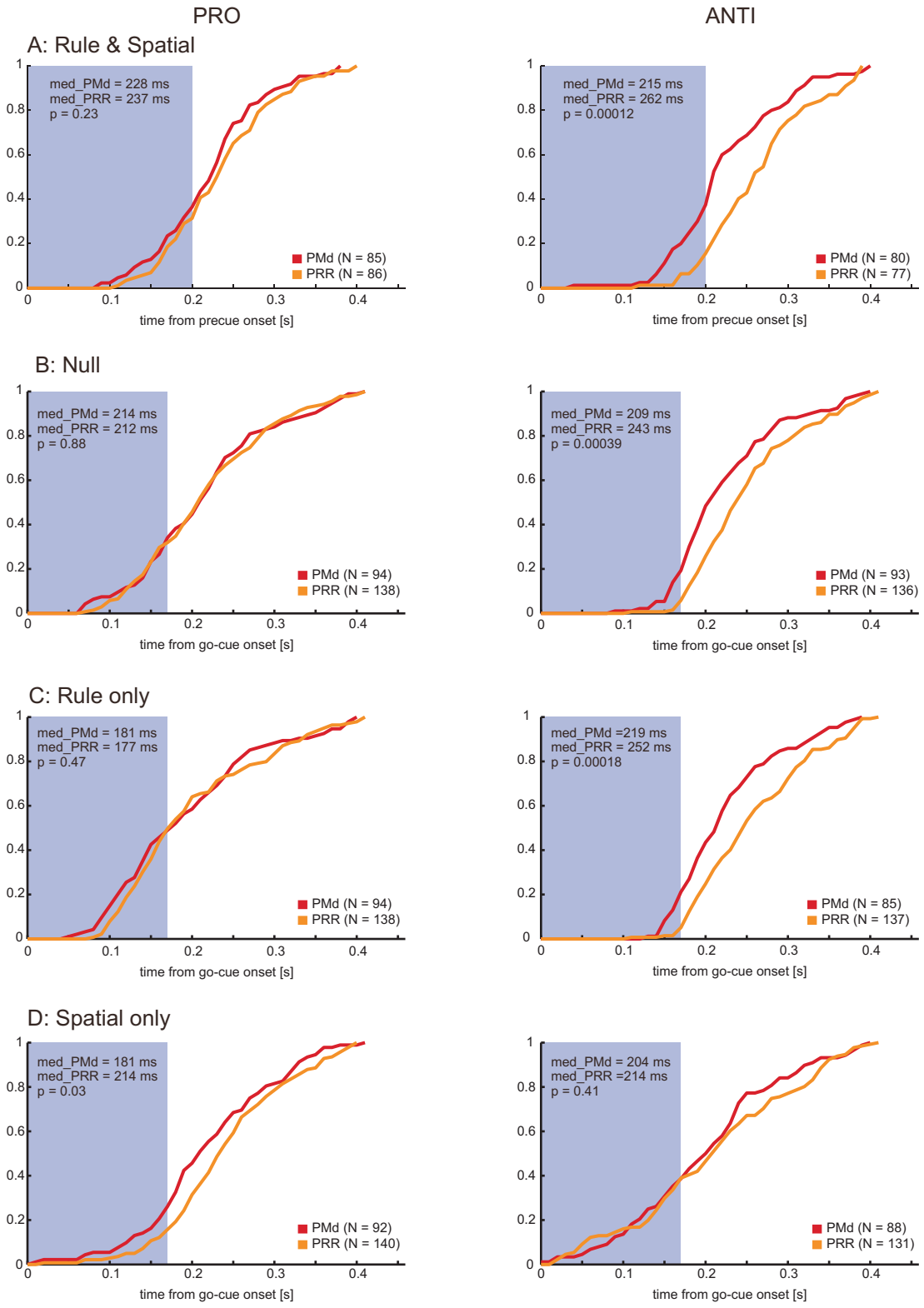

Figure S-3: Alternative neural latency measure. The curves show cumulative sums over the onset latencies of motor-related tuning. PMd (dark) and PRR (light) data are shown separately for pro- (left) and anti-trials (right) in the different cueing conditions (A-D). The motor-tuning onset latencies are derived for each single neuron within each condition. Additional to the cumulative sums the median onset latency and the p-value (ranksum-test) for the comparison between PMd and PRR onset latency distribution are provided. Also, the numbers of neurons in each area are provided, for which an onset latency could be computed.

Figure S-4

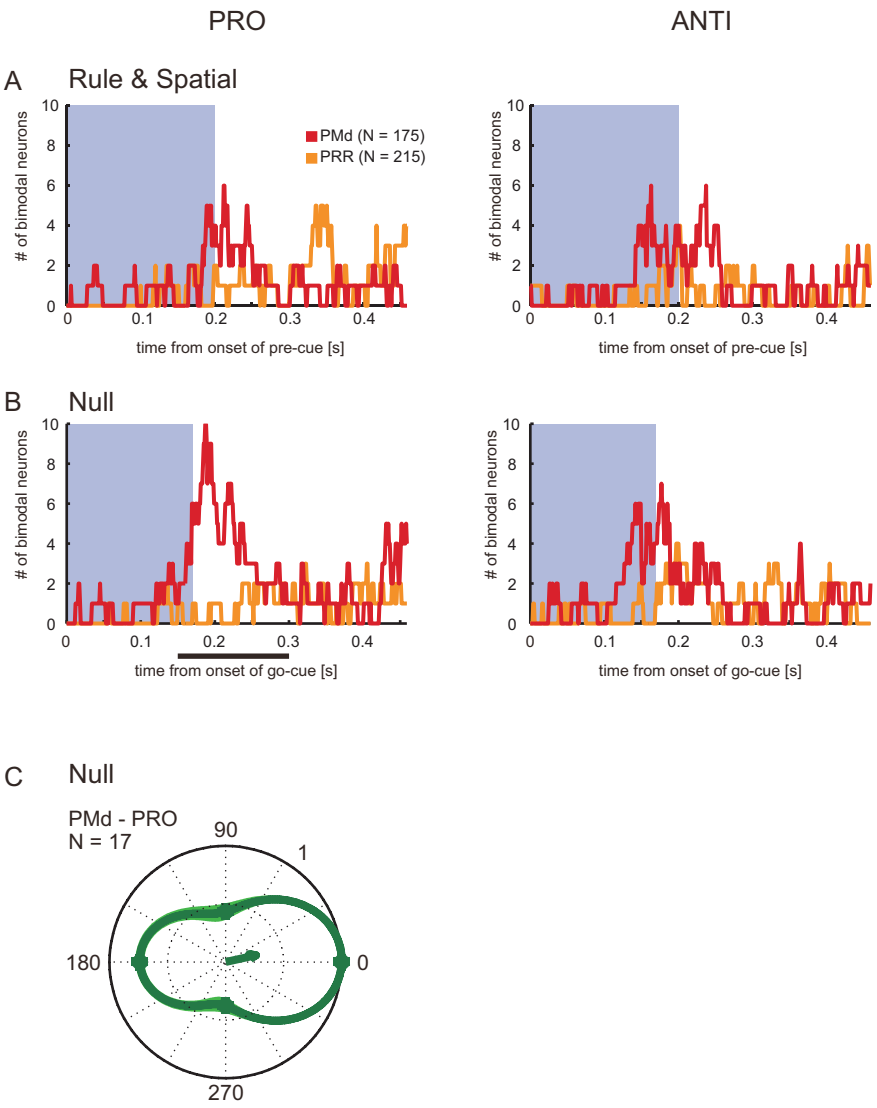

Figure S-4: Analysis of temporary bimodal tuning after cue presentation. A: Number of putatively bimodal neurons in PMd (dark) and PRR (light) and separate for pro- (left) and anti-trials (right) in the RS-condition after onset of the precue. B: Same as in A, but in the N condition after onset of the go-cue. C: Average normalized tuning of putatively bimodal PMd neurons in pro-trials in the N condition (the condition with the strongest indication for bimodal tuning). The tuning curve is bi-lobed, indicating bimodal tuning, even though not fully symmetrically. The time window, which was used for computing the directional tuning, is indicated by the black bar in B. Data are aligned and normalized to the average maximal response in pro-trials in the time window of analysis.